THE JOURNAL OF PHYSICAL CHEMISTRY B

Article

pubs.acs.org/JPCB

Conformational Diversity of the Helix 12 of the Ligand Binding Domain of PPARγ and Functional Implications

Mariana R. B. Batista and Leandro Martínez*

Department of Physical Chemistry, Institute of Chemistry, University of Campinas, CP 6154-13083-970, Campinas, SP Brazil

ABSTRACT: Nuclear hormone receptors (NR) are transcription factors that activate gene expression in response to ligands. Structural and functional studies of the ligand binding domains (LBD) of NRs revealed that the dynamics of their C-terminal helix (H12) is fundamental for NR activity. H12 is rigid and facilitates binding of coactivator proteins in the agonist-bound LBD. In the absence of ligand, H12 exhibits increased flexibility. To provide a comprehensive picture of the H12 conformational equilibrium, extensive molecular dynamics simulations of the LBD of the PPARγ receptor in the presence or absence of ligand, and of coactivators and corepressor peptides, were performed. Free-energy profiles of the conformational variability of the H12 were obtained from more than four microseconds of simulations using adaptive biasing-force calculations. Our results demonstrate that, without ligand, multiple conformations of the H12 are accessible, including agonist-like conformations. We also confirm that extended H12 conformations are not accessible at ordinary temperatures. Ligand binding stabilizes the agonist H12 conformation relative to other structures, promoting a conformational selection. Similar effects are observed with coactivator association. The presence of corepressor peptides stabilizes conformations not allowed in the ligand-free, Rosiglitazone-bound or coactivator-bound LBDs. Corepressor binding, therefore, induces a conformational transition in the protein. Nevertheless, initial stages of corepressor dissociation could be induced by the ligand as it stabilizes the H12 in agonist form. Therefore, the present results provide a comprehensive picture of the H12 motions and their functional implications, with molecular resolution.

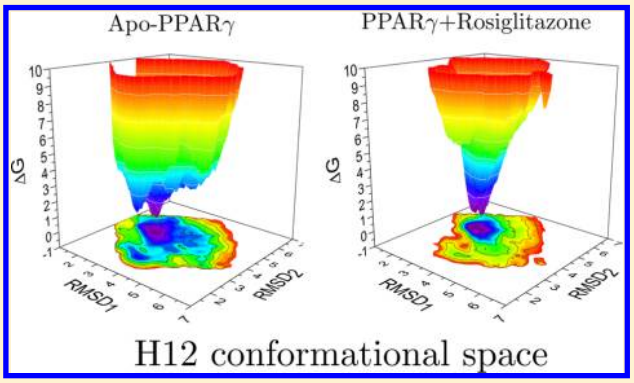

1. INTRODUCTION

Nuclear hormone receptors (NRs) are transcription factors modulated by ligand binding. Most NRs share the same overall architecture, consisting in three domains: a variable N-terminal domain, a well-preserved DNA binding domain (DBD), and a C-terminal ligand binding domain (LBD). Ligand binding can modulate transcription by controlling the structure and dynamics the LBDs. The LBDs of different receptors share similar structures, composed by about 12 helices which are packed in three approximately perpendicular layers, forming an α-helical "sandwich".[1,2] In the majority of crystallographic models obtained so far, the ligands are completely buried in the LBDs, such that some dynamical behavior is expected for ligand binding and dissociation, at least. Furthermore, many receptors are able to promote transcription even in the absence of ligand, suggesting that the structures of the LBDs mediating each functional response exist in a dynamical equilibrium, which exists independently but is affected by ligand binding.[3]

The rearrangement of the LBDs that is mostly associated with the functional response of the receptors involves its C-terminal helix, the Helix 12 (H12). The conformation of the H12 is determinant for the exposure of interaction sites for coactivator and corepressor proteins. In the presence of agonist ligands, the LBDs recruit coactivator proteins, initiating the signal cascade leading to target gene transcription. On the other side, in the absence of ligand or in the presence of antagonists, the conformation of the H12 favors the interactions of LBDs with corepressor proteins, which suppress the target genes.

The conformational variability of the H12 is, therefore, one of the fundamental aspects governing NR function. The dynamic nature of this helix was recognized early with the determination of crystal structure of ligand-bound (holo) and ligand-free (apo) retinoic acid receptors. While the structure of the apo-retinoic X receptor-α (RXRα)[4] displayed an extended H12 not contacting the body of the LBD, the holo-retinoic acid receptor-γ[5] was found with the H12 packed over the LBD in a compact form. This notable difference suggested originally that the LBDs of NRs would exist in a stable apo conformation in the absence of ligand which would shift to the compact holo structure upon ligand binding.[6−8]

There are two general models for the mechanisms a ligand can affect the function of a biological macromolecule. The first model, known by "conformational selection", describes an intrinsically dynamic protein in the presence or absence of the ligand. The ligand binds to a subset of the conformations, shifting the equilibrium toward this subsets and, thus,

Received: October 7, 2015
Revised: November 23, 2015
Published: November 23, 2015

DOI: 10.1021/acs.jpcb.5b09824
J. Phys. Chem. B 2015, 119, 15418−15429

modulating the activity. The bound state, therefore, is a subset of conformations which is stabilized by ligand binding, although these same conformations are populated in the absence of the ligand.[9] By opposition, the "induced fit" model assumes that the bound state is characterized by conformations which are not sampled in the absence of ligand. Ligand binding promotes a conformational transition from the unbound to the bound state.[9−11] Simplified representations of these models are shown in Figure 1.

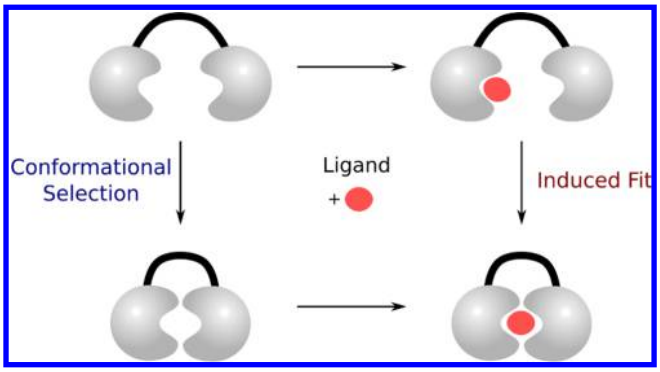

Figure 1. Sketch of the two models describing the role of ligands in the conformational equilibrium of receptors. In the conformational selection mechanism, the ligand binds a subset of conformations which are populated even in the absence of ligand, and stabilizes this subset which is identified as the bound state. In the induced fit mechanism, the conformational transition to the bound state occurs after ligand binding and is promoted by it.

The large conformational shift observed for the H12 in the first crystallographic models was consistent with an induced-fit mechanism. The LBD, therefore, should exist in a stable apo form which could suppress gene transcription, and be transformed upon ligand binding to the holo active form. The fundamental conformational change should involve the H12 and the exposure of coactivator or corepressor interaction surfaces.

Nevertheless, the evidence for the induced-fit mechanism were not supported by further functional and structural data.[12,13] For instance, no other apo-LBD models were found in which the H12 assumed the conformation observed for RXRα, unless when induced by crystallographic packing.[14] Crystallographic apo-LBD models, on the other side, were obtained in a compact form, similar to holo-RXRγ, for the ligand-free Peroxissome-activated activated receptor-γ (PPARγ),[15] estrogen receptor-γ (ERγ),[16] and for orphan receptors. Additionally, hydrogen−deuterium exchange experiments have shown that the H12 protects the surface of the thyroid hormone receptor (TR) LBD even in the absence of ligand.[17] Finally, many receptors, such as PPARγ, display basal activity; that is, they promote gene transcriptions and thus allow the recruitment of coactivator proteins, also without ligand.

Molecular dynamics (MD) simulations further supported the possibility of a more subtle conformational equilibrium of the H12 of NR LBDs. For instance, our group and others have shown that ligand binding and dissociation routes do not seem to involve major displacements of the H12.[12,18−23] More recently, we demonstrated that the experimentally observed fluorescence anisotropy decay rates of a probe bound to the H12 of PPARγ are consistent with an H12 which is persistently bound to the body of the LBD.[24] Therefore, no large conformational changes should be expected for the H12.[24] Additionally, extended MD simulations performed by Fratev[25] have shown that extended H12 conformations are not favorable for the estrogen receptor and that the H12 equilibrium between agonist and antagonist conformations is subtly affected by receptor dimerization.

Experimental and computational evidence, therefore, is suggesting that the activation of the NR LBDs is of the conformational-selection type. The receptors, or more specifically the LBDs, appear to sample both apo and holo conformations, which might be preferentially stabilized by ligand binding. The most promising target for computational studies of this conformational equilibrium is the LBD of PPAR receptors. PPAR crystallographic models were obtained in the apo form, in the holo form with coactivator peptides bound (Figure 2A), and in the form bound to both antagonists and

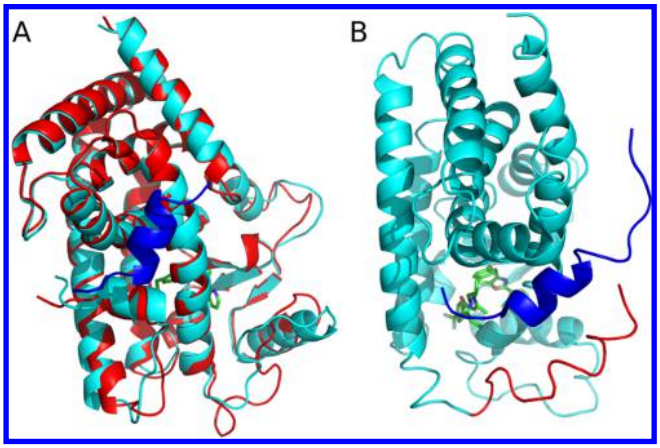

Figure 2. Crystallographic models for PPARγ. (A) Superposition of the LBD of PPARγ in the presence (cyan) or absence (red) of the natural ligand Rosiglitazone. (B) Crystallographic models of PPARα bound to an antagonist ligand and a corepressor peptide. The coactivator and corepressor peptides are colored in blue.

corepressor peptides (Figure 2B).[15,26] Therefore, the conformational variability of the receptor induced, or favored, by each set of ligands and cofactors is relatively well-known.

In this work, we aim to describe in details the conformational equilibrium of the H12 of PPARγ. We perform extensive MD simulations with modern free energy calculation methods to obtain a comprehensive profile of the stability of the LBD as a function of the conformations probed by the H12 in various conditions. We show that the free energy barriers involved are consistent with a conformational-selection model for ligand and coactivator action, and an induced-fit model for corepressor binding. No extended or highly displaced H12 conformations are accessible at ordinary temperatures. Therefore, we provide a comprehensive description of the possible movements of the most significant transcription activation switch of PPARγ, that is probably valid for other NRs.

MATERIALS AND METHODS

Molecular Dynamics simulations were performed for the LBD of PPAR starting from the crystallographic models 2PRG[15] or 1KKQ,[26] for the representation of apo, holo, cofactor free, coactivator-bound, and corepressor-bound PPAR LBD, as will be discussed.

DOI: 10.1021/acs.jpcb.5b09824
J. Phys. Chem. B 2015, 119, 15418−15429

In all cases, the structures were solvated with Packmol[27,28] with about 22 thousand water molecules, and sodium and chloride ions to render the system neutral. Simulations were performed using the CHARMM27 force-field[29] for the protein and peptides, the parameters described by Anders et al.[30] for Rosiglitazone, and the TIP3P model for water.[31] All energy minimization steps and simulations were performed with NAMD.[32] Equilibration and simulations were performed in the NPT ensemble at 298.15K and 1 atm using a time-step of 2 fs. Covalent bonds involving hydrogen atoms were kept rigid according to standard protocols. Temperature was controlled using Langevin dynamics with a friction coefficient of 10 ps^{-1}. The Nosè-Hoover algorithm was used for pressure control, with a piston oscillation period of 200 fs and decay rate of 100 fs. Long-range electrostatic interactions were computed with the PME method. A cutoff of 12 Å was used for van der Waals interactions.

The systems were equilibrated with (1) 1000 steps of conjugate-gradient (CG) energy minimization followed by 200 ps MD keeping all protein, ligand and cofactor atoms fixed, for solvent relaxation. (2) 500 CG minimization steps followed by 200 ps MD with fixed Cα coordinates, allowing the side-chains of the protein to relax. (3) 2 ns MD without any restrictions. The final structure of this last MD was used for production runs.

The Rosiglitazone and coactivator bound crystallographic structure of PPARγ (2PRG) was used for the construction of the models for (1) apo-PPARγ, for which the ligand and the coactivator peptide were removed, (2) holo-PPARγ, for which only the coactivator peptide was removed, and (3) ligand-free, coactivator bound PPARγ, for which only the ligand was removed from the crystallographic model. The PPARα (1KKQ) crystallographic model was used for the simulation of the corepressor-bound LBD, so the antagonist ligand was removed.

VMD was used for visualization and figure preparation.[33] Cpptraj from the AmberTools 14 suite was used for RMSD-based conformational clustering of the structures by means of a hierarchical algorithm.[34,35] The most representative structure of each cluster was obtained by Cpptraj and used to produce figures. Different RMSD criteria for the definition of the clusters were tested, and the one that provided the most clear discrimination of clusters was considered.

Adaptive Biasing-Force Simulations. All simulations performed here aimed the comprehensive profiling of the free energies involved in conformational transitions of the H12 of the LBD. The adaptive biasing-force (ABF) algorithm was chosen for mapping the free energies along reaction coordinates involving displacements of the H12 of the LBD under different conditions. The ABF method is currently one of the most efficient strategies for accelerated conformational sampling in MD simulations.[36,37]

Briefly, ABF is a strategy for accelerated sampling and free energy profiling along a reaction coordinate. Given a reaction coordinate ξ that can be defined in terms of the coordinates of the atoms of the system, the ensemble average force acting on the atoms at ξ provides the gradient of the free energy.[37] Therefore, if an effective sampling of conformations is performed within the range of ξ of interest, the free energy profile relative to any reference state can be reconstructed from the average force.

The ABF method consists on performing MD simulations in which the average force acting on atoms that define the reaction coordinate of interest is computed. Once the average force on each atom is adequately estimated for a given reaction coordinate ξ, a force with same modulus but with opposite direction is added to the system whenever it samples that same reaction coordinate. From then on, the forces acting along the reaction coordinate at that point will be on average null, and the system will move diffusively. When a diffusive motion along the complete reaction coordinate of interest is obtained, the free energy profile along it can be obtained from the biasing force which was introduced. More detailed descriptions of the method with rigorous justifications can be obtained elsewhere.[36−40]

In ABF simulations, therefore, it is fundamental to define an adequate reaction coordinate. Here, we aimed to study the conformational variability of the H12 of the LBD of PPAR receptors, therefore the reaction coordinate should represent displacements of this helix. The RMSD of the helix relative to some conformation of choice would be, therefore, the natural choice. However, many different conformations might display the same RMSD relative to a single reference structure, such that the free energy computed for that RMSD would not be representative of a well-defined subset of conformations. This problem is greatly reduced if multiple reference coordinates are used.[40] That is, if the reaction coordinate is defined as the RMSDs relative not to one, but to multiple structures. The reaction coordinate then becomes multidimensional. A complication arises, then, on the definition of the multiple reference coordinates.

Here, ABF simulations were used first as an auxiliary enhanced sampling method to obtain different reference coordinates, than as the tool to map the multidimensional free energy profile. The first set of simulations consisted in ABF simulations in which a single reference structure was used, i.e., the H12 conformation present in the crystallographic model. The conformational variability of the H12 in this simulation was used to obtain an alternative conformation displaying the largest displacements from the crystallographic model, but preserving the secondary structure of the helix. Using this new H12 conformation and the conformation observed in the crystallographic structure, the multidimensional free energy profiles were obtained.

The ABF simulations were performed as implemented in NAMD.[32] In the auxiliary simulations performed for mapping H12 conformations, the reaction coordinate was defined as the RMSD relative to the agonist H12 conformation of 2PRG. The ABF force was applied only on the loop connecting helices 11 and 12, because its application on all residues of the H12 promoted a rapid disruption of the secondary structure instead of the effective displacement of the helix. The RMSD of this loop was sampled by ABF simulations within 1 and 10 Å, with a precision of 0.1 Å. The movements of the atoms outside the region of interest were avoided by the use of an harmonic boundary potential with a 10 kcal mol^{-1} $Å^2$ force constant. Four independent 80 ns ABF simulations were performed with this protocol, and as mentioned above the H12 of largest displacement, but preserving the secondary structure, was selected, for the productive ABF simulations that followed. The agonist H12 conformation and the alternative conformation selected are represented in Figure 3.

Production ABF runs used the two reference structures to define a multidimensional reaction coordinate based on the RMSDs of the H12 relative to both models. The two models will be referred as the "agonist conformation", obtained from

DOI: 10.1021/acs.jpcb.5b09824
J. Phys. Chem. B 2015, 119, 15418−15429

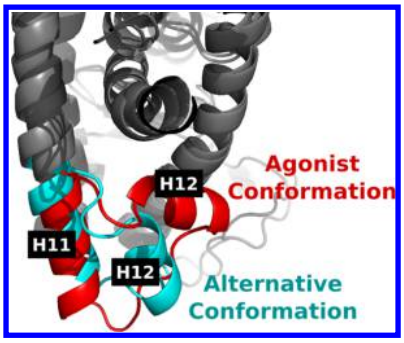

Figure 3. Agonist and alternative conformations used as reference structures in the multidimensional ABF simulations.

the holo-PPARγ crystallographic structure, and the "alternative conformation", obtained from the auxiliary ABF run (Figure 3). The RMSDs defining the reaction coordinates were computed for Cα atoms of residues 449 to 477, containing the C-terminal end of the H11, the loop between H11 and H12, and the H12. The same range of RMSDs, precision and boundary potentials of auxiliary ABF run were used. However, the sampling here was exhaustive. The minimum sampling time for the force at each reaction coordinate was 1 ps.

For the apo-PPARγ and the Rosiglitazone-bound PPARγ models, a total of 1.2 μs of ABF simulations were performed to guarantee convergence of the free energy profiles. These simulations were divided in 12 sets of 100 ns each. For the corepressor-bound and coactivator-bound models, 1.0 μs of ABF simulations was performed. The convergence of the free energy profiles was probed by computing the average deviation of the free energies predicted at the regions of low free energy. The profiles were considered to be converged if the deviation of the free energy resulting from the removal of any set of 100 ns simulation was in average smaller than 0.5 kcal mol^{-1} in all regions differing from the free energy minimum by less than 4 kcal mol^{-1}.

RESULTS AND DISCUSSION

Accessible Conformations of PPARγ H12. The free energy profiles of ligand-free and ligand-bound PPARγ are shown in Figure 4. The first noticeable difference between the free energy surfaces of parts A and B of Figure 4 is that in the ligand-free model there is a larger region of low free energies, and two clearly discernible local minimizers. The free energy surface of the ligand bound model (Figure 4B), on the other side, displays a much more narrow low-energy well. At the same time, the global minimizers of the free energy have similar positions in both plots.

The large well in which the global minimizer of the ligand-free receptor is found is composed by many local minimizers that differ in energy by less than ∼4 kcal mol^{-1}. At 298.15 K, each increase of ∼1 kcal mol^{-1} in the free energy represents a decreased 80% probability of observation of the higher energy state. Therefore, ∼ 4 kcal mol^{-1} represents an upper limit the observable energy states at room temperature, with about 0.1% probability. States differing in energy in less than ∼3 or ∼4 kcal mol^{-1} from the state that globally minimizes the free energy are significantly populated at room temperature. Therefore, the blue and cyan regions of lower energy observed in the free energy surfaces of Figure 4 are accessible at room temperature, and illustrate the range of conformations that the H12 can assume. The wider free energy well of the ligand-free PPARγ model clearly indicates a greater conformational variability relative to the ligand-bound model. This was expected and confirms the greater flexibility of H12 in the absence of ligands.[41−44] The present simulations allow the actual structural characterization of the accessible conformations.

The global free energy minima for both ligand-free and Rosiglitazone-bound simulations was found close to the $RMSD_1$ = 3 Å and $RMSD_2$ = 4 Å reaction coordinate. The conformations in the proximities (±0.1 Å) of these regions were clustered in each system, and the most populated representative structures were identified. These structures are shown in Figure 5A and B, superposed to the crystallographic holo-PPARγ model. The most populated position of the H12 on both ligand-free or ligand-bound free energy minima differs only slightly from the H12 observed in crystallographic models of the ligand-bound PPARγ. In this conformation, the H12 is perpendicular to H3, and attached to the body of the LBD by a network of hydrogen bonds which is similar to the one observed for the ligand-bound structure (Figure 5C). These interactions involve residues Glu324 (from the loop between H4 and H5), Arg397 (loop within H8 and H9), Arg443 (from H11), and Tyr477 (from H12).[45] Interestingly, it was already demonstrated that the mutation of these residues to Alanine reduces significantly the basal activity of PPARγ, thus supporting their stabilization of the active H12 conformation even in the absence of agonist ligands.[46,47]

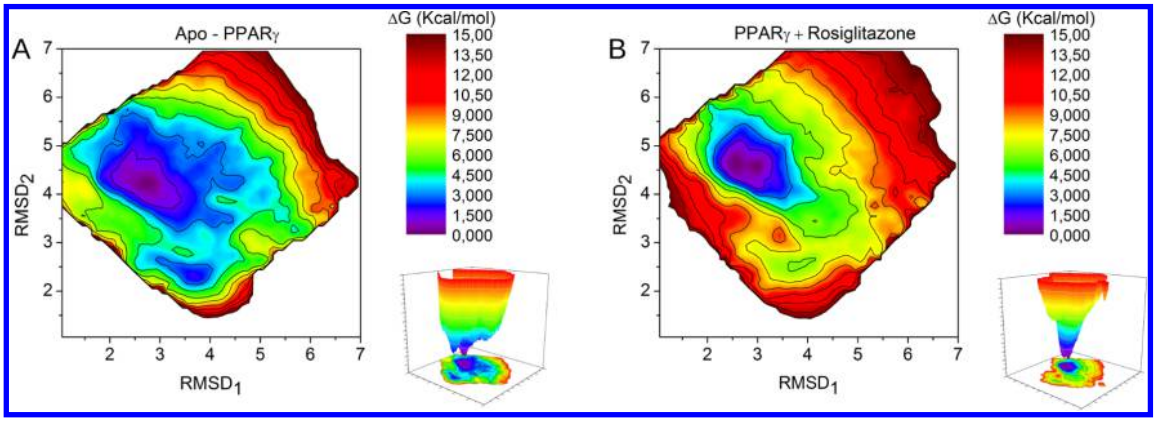

Figure 4. Free energy surfaces of the conformational variability of the H12 of PPARγ. (A) Ligand-free LBD. (B) Rosiglitazone-bound LBD. The wider well of the ligand-free free energy surfaces implies a greater conformational variability.

DOI: 10.1021/acs.jpcb.5b09824
J. Phys. Chem. B 2015, 119, 15418−15429

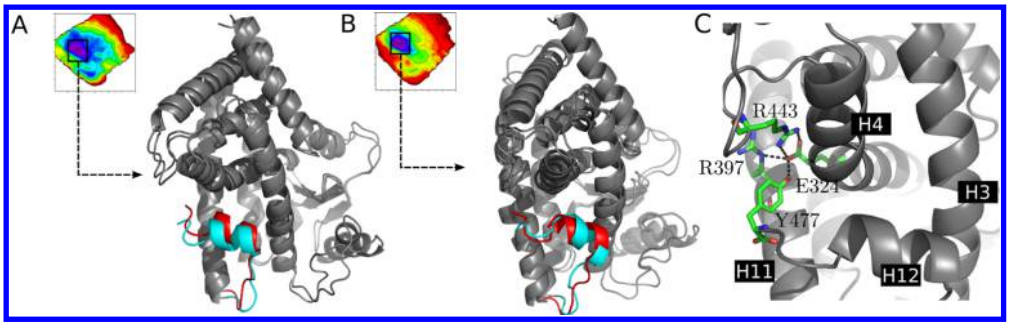

Figure 5. Comparison of the representative conformations of the free energy minima (cyan) and the crystallographic model of holo-PPARγ[15] (red) for (A) ligand-free PPARγ simulations and (B) Rosiglitazone-bound PPARγ simulations. (C) Detailed view of the interactions that stabilizes H12 in active conformation.

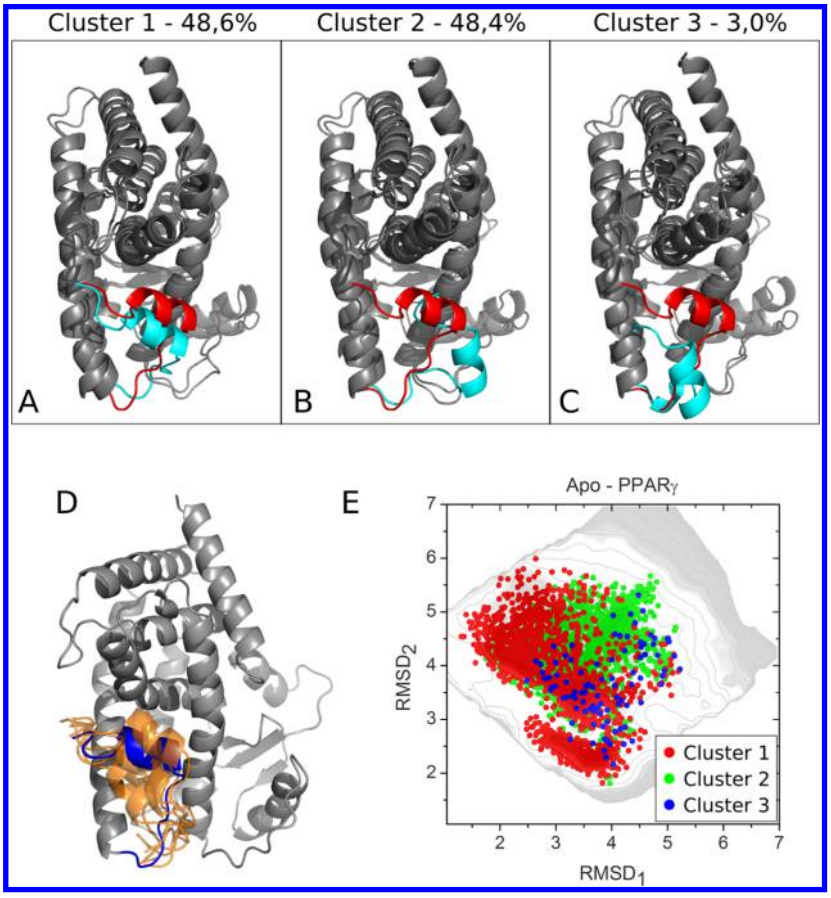

Figure 6. Most representative conformations of the H12 obtained by clustering analysis of the ligand-free PPARγ ABF simulation. In all figures, the crystallographic model of holo-PPARγ is depicted in red. (A) Representative structure of the most populated cluster. (B) Representative structure of the second most important cluster. (C) Representative structure of the third and minor cluster. (D) Representation of the conformational variability experienced by the H12 in cluster **1**. The conformation of the global free energy minimizer is depicted in blue. (E) Acessible conformations selected to clustering analysis: the red, green, and blue points indicate the confomations of clusters **1**, **2**, and **3**, respectively.

Naturally, the basal activity depends on the association of a coactivator protein. Indeed, the position of the most relevant residues responsible for the establishment of the coactivator binding surface are also preserved in the ligand-free global free energy minimum. For instance, the interactions of the coactivator peptide SRC-1 depend on the relative positions of residues Lys301 (from H3) and Glu471 (from H12), and the mutation of these two residues to alanine can decrease in about 30% the basal activity of the receptor.[46]

Therefore, our simulations indicate that the basal activity of PPARγ can be consistently associated with LBD conformations which are similar to the ones assumed by the receptor upon ligand binding. Furthermore, these conformations are not only accessible, but even in the absence of ligand they comprise the free energy minimum and, therefore, remain as the most populated set of conformers of the H12. This observation justifies the fact that, particularly for PPARs, structures in active form were obtained with a great variety of ligands and even without ligands,[15,48−50] while different H12 conformations were experimentally obtained only when the H12 is displaced by corepressor binding proteins.[26]

However, without ligand, the active conformation of H12 competes with multiple conformations that have slightly higher energies and are accessible at ordinary temperatures. Thus, the

DOI: 10.1021/acs.jpcb.5b09824
J. Phys. Chem. B 2015, 119, 15418−15429

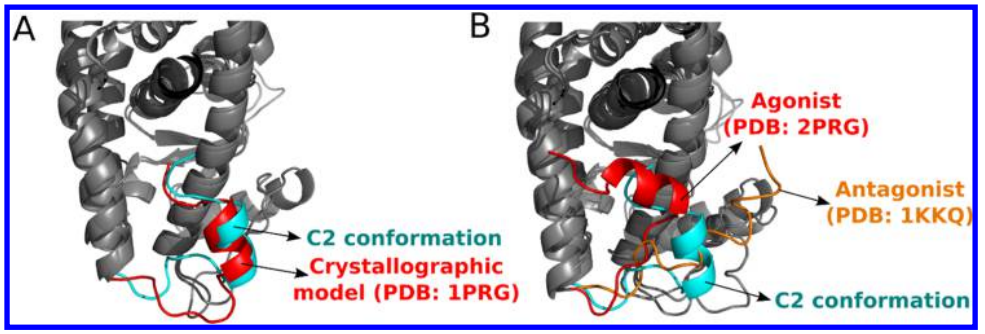

Figure 7. (A) Superposition of the crystallographic model obtained by Nolte et al.[15] (red) and of the representative structure of the second most important cluster (cyan). (B) Superposition of the agonist crystallographic model (red), antagonist crystallographic model (orange), and the C2 conformation (cyan).

conformational variability of the H12 in the ligand-free LBD was studied by clustering the structures sampled by the ABF simulation. Conformations which displayed free energies not greater than 4 kcal mol^{-1} than the global minimizer were considered to be accessible at room temperature. The clustering was performed using pairwise RMSDs as the similarity measure. The conformations can be clearly discriminated in three clusters. Two of the clusters responded to roughly 97% of the conformations. The mean free energy difference between the two most populated cluster is of only ~0.2 kcal mol^{-1}. A third minor set of structures was classified separately. The most representative conformations of each cluster are shown in Figure 6A–C, aligned to the holo-PPARγ crystallographic model. Figure 6D represents the conformational variability of the most significant cluster, and Figure 6E shows the distribution of the conformations of each cluster on the free energy surface. It is important to remark that the RMSDs resulting from clustering analysis are not necessarily the same as the ones that define the reaction coordinate, so that there is overlap on the distributions of the structures of each cluster on the free energy surface (Figure 6E).

The most representative structure of cluster **1** (Figure 6A-cyan) shows that it groups H12 conformations which are similar to that of the crystallographic holo-PPARγ (Figure 6A-red). The most populated cluster, therefore, contains the global free energy minimum, and is characterized by local fluctuations of the H12 around the agonist conformation, which allows the recruitment of coactivators (Figure 6D).

A representative structure of the second most populated cluster of conformations is shown in Figure 6B. This conformation will be referred to as the C2 conformation from now on. The H12 is clearly displaced from the agonist conformation, being almost parallel to H3. In the C2 conformation, the H12 blocks the access to hydrophobic residues Thr297, Leu311, Gln 314, Val315, Leu318 and Leu468 and to the hydrogen bonding Glu471, that form the coactivator binding surface. Therefore, this H12 blocks coactivator recruitment and is, consequently, inactive.

This conformation is remarkably similar to the crystallographic structure obtained by Nolte et al. (PDB: 1PRG[15]) for chain B of the PPARγ without ligand, as shown in Figure 7A. Therefore, the most important conformations of H12 observed in the ABF simulations are consistent with the experimental H12 conformations. The present results show that, in the absence of ligand, these conformations are significantly populated, and are separated from the minimum free energy structure by ~2.5 kcal mol^{-1}. Thus, our results support the structure of Nolte et al. as a representative structure of apo-PPARγ in solution, and not simply a crystallographic artifact. At least, it is a conformation which might have been stabilized by crystal contacts, not induced by them, thus possibly being functionally relevant. The C2 conformation is also half way from the agonist to the antagonist conformation observed for corepressor-bound PPARγ, such that transitions from this conformation to one or other state can be thought to be facilitated upon binding of agonists, antagonists, or cofactor proteins (Figure 7B).

The binding site accessibility is different depending on the conformation of the H12. When H12 assumes the agonist conformation, it blocks access to the binding pocket, as shown in Figure 8A. On the other side, the C2 conformation creates

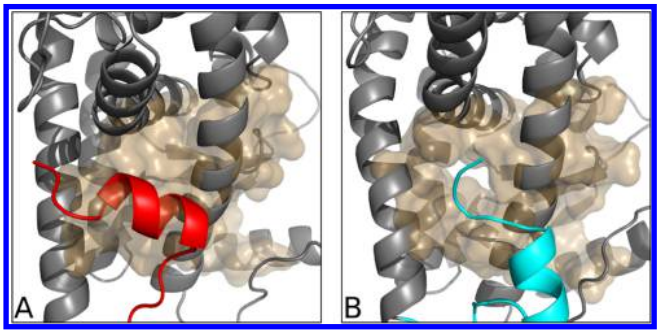

Figure 8. Binding site cavity of (A) agonist and (B) C2 conformation.

an aperture at the surface of the binding cavity which might permit the access of the ligand, as shown in Figure 8B. Therefore, the C2 conformation might be important for ligand binding and dissociation. Displacements of the H12 observed in MD simulations of ligand dissociation from the LBD of other receptors are consistent with movements of this magnitude.[18−21]

Finally, the representative conformation of cluster 3 (C3 conformation) displays the H12 far from the agonist conformation, exposing the binding pocket (Figure 6C). This conformation is less populated than others, but is also accessible, and it could be important for facilitating ligand binding or dissociation. It could also be stabilized by ligands in intermediate association or dissociation stages. It is not, however, consistent with the binding of coactivators nor corepressors, such that it might not have any functionality other than providing accessible intermediates for structural transitions between functional states.

Rosiglitazone Stabilizes the Agonist H12 Conformation. ABF simulations of PPARγ without ligand revealed the

DOI: 10.1021/acs.jpcb.5b09824
J. Phys. Chem. B 2015, 119, 15418−15429

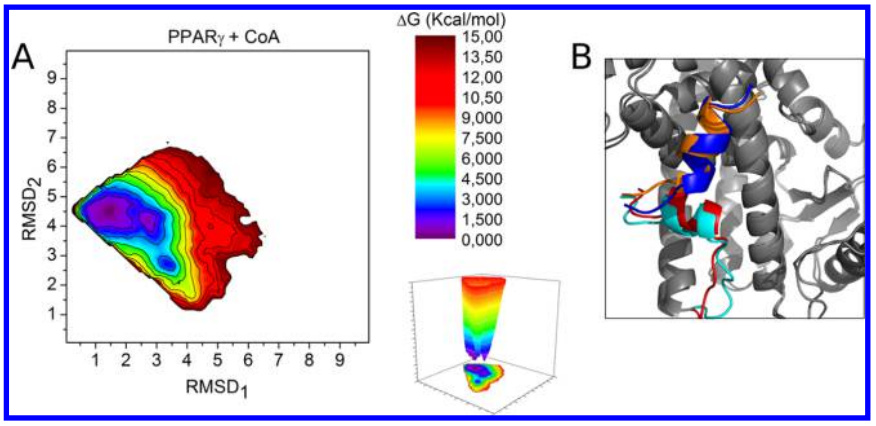

Figure 9. (A) Free energy surface of the conformational equilibrium of H12 of PPARγ in the absence of ligand, but bound to a coactivator peptide. (B) Comparison of the representative conformations obtained via ABF simulation (cyan and blue) and the experimental structures (red and orange).

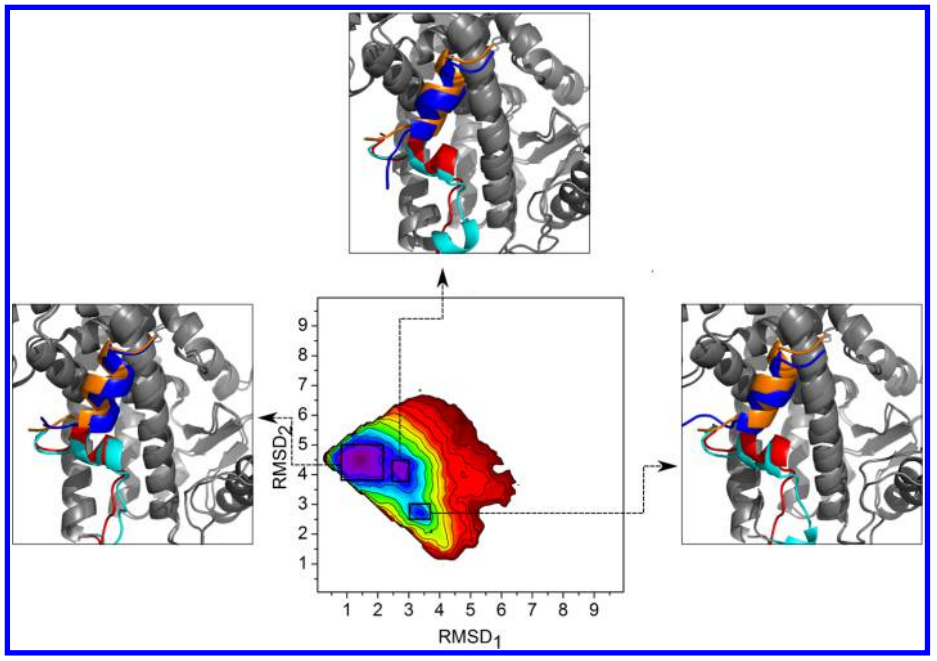

Figure 10. Representative conformation of each local minimum observed in coactivator-bound ABF simulations. The structures exhibit the H12 in a conformation corresponding to the agonist conformation, which is greatly stabilized by coactivator binding. Crystallographic models (red and orange) and simulation models (cyan and blue) are shown.

existence of a set of conformations of the H12 which are accessible at ordinary temperatures. These conformations can be clustered into three sets, where the two most populated clusters comprise about 97% of the conformations observed. A representative structure of the most populated conformer is similar to the agonist H12 conformation. The second most populated conformer is displaced from the agonist conformation, and is similar to one of the H12 conformations observed in chain B of apo-PPARγ crystallographic models.[15]

When Rosiglitazone, an agonist ligand, is present, the free energy surface changes significantly, as can be observed in Figure 4. It is clear from Figure 4B that with Rosiglitazone bound, the global free energy minimum is found in a narrow well with much lower free energy than any surrounding conformation. The ligand, therefore, stabilizes significantly the global free energy minimum relative to other conformations, and only structures which belong to the same free energy well can be significantly populated at room temperature.

The global free energy minimizer is, not surprisingly, very similar to the agonist H12 conformation observed in crystallographic models of PPARγ bound to various agonist ligands, as shown in Figure 5B. It is also similar, therefore, to the global free energy minimizer of the ligand-free ABF simulation. However, only small perturbations are thermodynamically allowed in the ligand-bound state. Clustering of the accessible conformations in this simulation results in a single dominant cluster comprising essentially all the structures, for which the agonist H12 conformation is a good representative.

These results are, as a whole, quite consistent with the qualitative picture that has emerged for the flexibility of H12 in solution, from experimental data: In the absence of ligand, the H12 is flexible, and able to assume the agonist conformation, conferring basal activity to PPARγ. However, we demonstrate, here, that the displacements of the H12 are relatively small, particularly if compared to the detachment of the H12 which was observed for the apo-RXR crystallographic model.[4] This

DOI: 10.1021/acs.jpcb.5b09824
J. Phys. Chem. B 2015, 119, 15418−15429

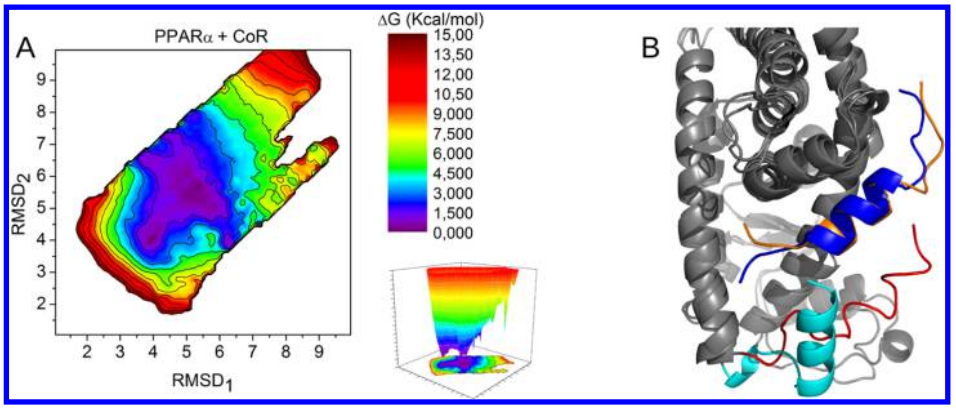

Figure 11. (A) Free energy surface of the conformational equilibrium of H12 of PPARα in the absence of ligand, but bound to a corepressor peptide. (B) Comparison of the representative structure of the minimum energy region (cyan and blue) and the antagonist crystallographic model (red and orange).

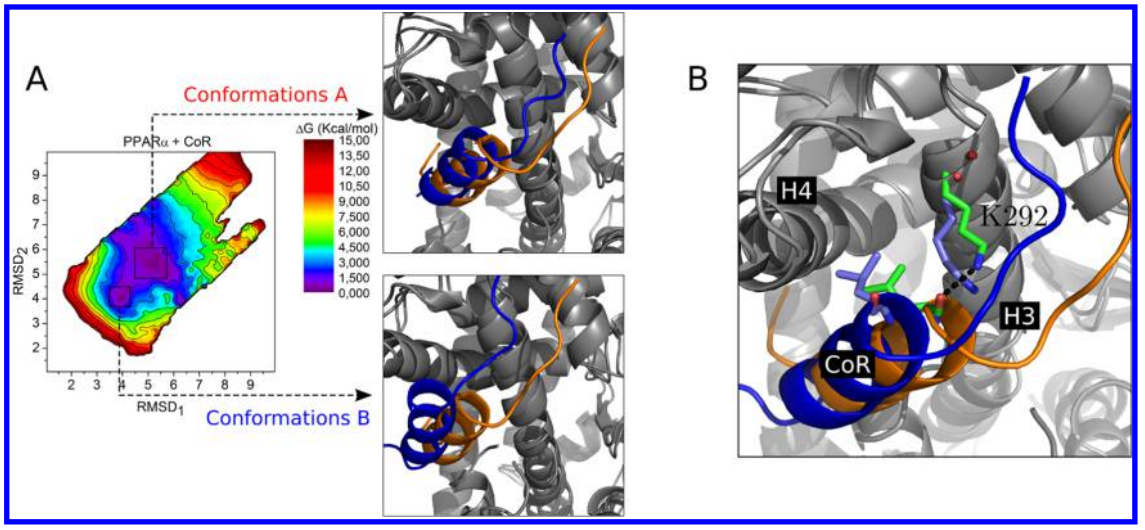

Figure 12. (A) Conformations of H12 similar to the agonist PPARγ model are observed (conformation B) with free energies not greater than ~2 kcal mol^{-1} than that of the global minimizer These conformations are associated with the displacement of the coactivator peptide, and suggest how the ligand actively promotes the dissociation of the corepressor. (B) Hydrogen bond (black dashed line) between SMRT CoR and PPARα. Crystallographic models (orange) and simulation models (blue) are shown.

confirms the interpretation of time-resolved fluorescence anisotropy decay experiments provided in previous works.[24,41]

In the presence of agonists, on the other side, the flexibility is greatly reduced, and the agonist conformation becomes the only significantly populated one. The ligand, therefore, performs a conformational selection within a range of configurations of the H12 which are accessible in the apo-receptor. The stabilization of the agonist conformation, of course, facilitates the recruitment of coactivator proteins.

The Role of Coactivators in H12 Conformational Equilibrium. In order to evaluate the role of coactivator proteins in the conformational equilibrium of the H12, ABF simulations in the presence of a coactivator peptide SRC-1[15] were performed. The free energy surface obtained is represented in Figure 9A.

The representative structures of accessible conformations of the H12 in the presence of the coactivator peptide are also agonist-like, as shown in Figure 9B (the dominant cluster comprises more than 99% of the structures). The stabilization of this conformation promoted by the coactivator is, however, stronger than that promoted by the ligand. The H12, in the minimum free energy conformation, forms the same interactions which are present in the previous simulations, but is further stabilized by direct interactions with the coactivator. Displacements from this conformation, with high energy, were observed in the ABF simulations, and are consistent with movements leading to the antagonist crystallographic PPARα H12 conformation. However, these displacements require the concerted dragging of the coactivator peptide and are unfavorable. The ligand and the coactivator, therefore, have complementary roles in the stabilization of the agonist H12 conformations.

Three free energy minima were observed in the presence of the coactivator peptide. However, the actual structures associated with these minima exhibit the H12 in conformations which are all very similar to the agonist conformation. Only small perturbations in the position of the loop connecting helices 11 and 12 are observed (Figure 10).

Therefore, the association of the coactivator has a strong stabilizing effect on the agonist conformation of the H12, which is more important than the stabilization promoted by Rosiglitazone alone. This suggests that the dynamical equilibriums of ligand binding, H12 rearrangement, and coactivator recruitment occur at different time-scales. The

DOI: 10.1021/acs.jpcb.5b09824
J. Phys. Chem. B 2015, 119, 15418−15429

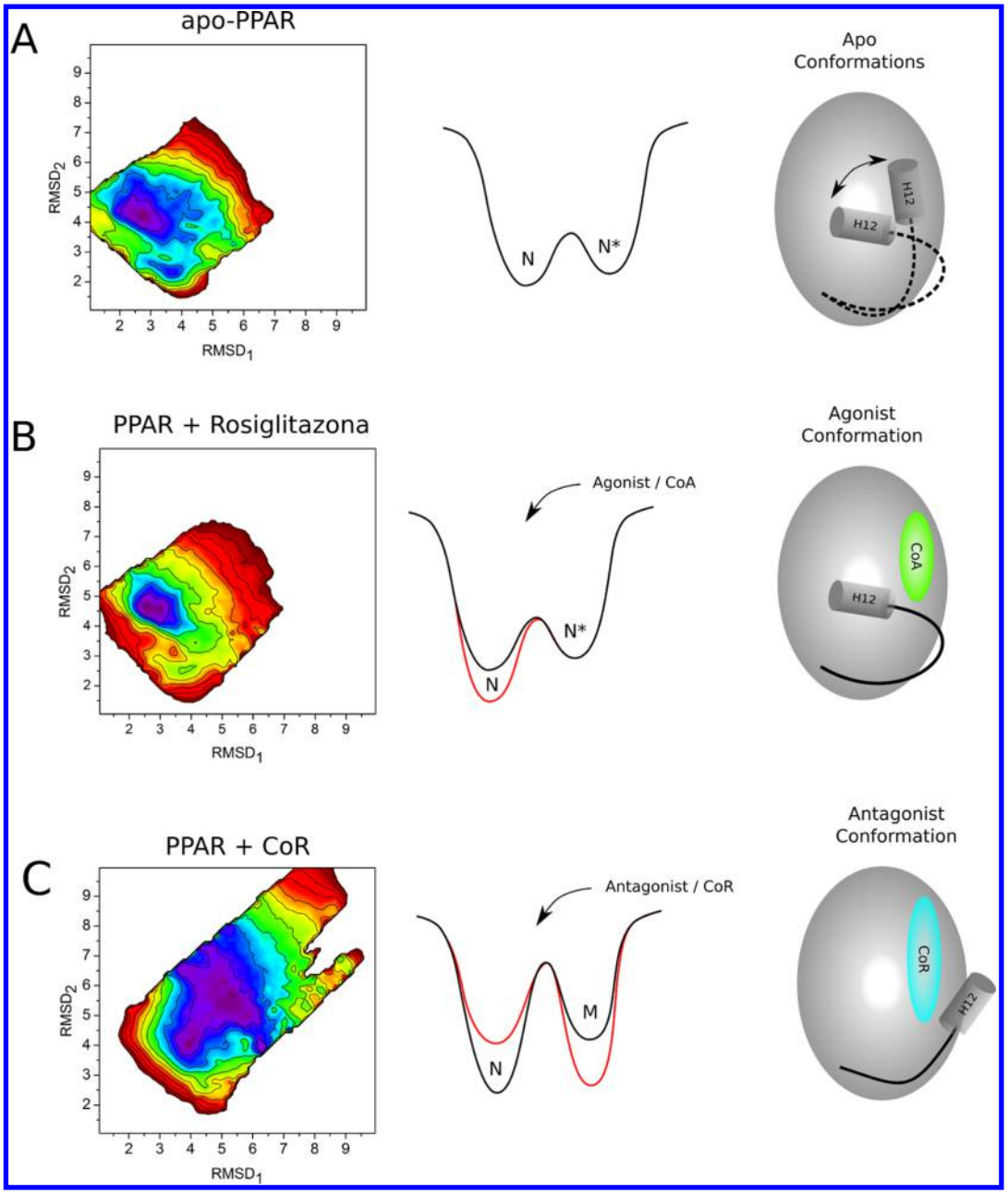

Figure 13. Sketch of the free energy profile and conformational equilibrium of H12: (A) In the absence of ligand, multiple conformations of H12 are accessible, with the agonist one being the most stable. (B) Ligand binding promotes a conformational selection and the agonist conformation is stabilized relative to other conformations. The association of the coactivator has a similar and probably additive effect. (C) Corepressor binding, on the other side, promotes a conformational transition of the H12 that cannot be explained by the accessible conformations of the ligand-free receptor.

most plausible scenario would involve ligand binding and dissociation from a coactivator-free receptor. With agonist binding, agonist H12 conformations are selected, favoring coactivator recruitment. With coactivator recruitment, this LBD conformation is further stabilized. The dissociation of the coactivator, then, becomes the limiting step for the restoration of the inactive receptor.

The Role of Corepressors in the Conformational Equilibrium of Antagonist H12 Conformations. Experimentally, the association of corepressors is associated with a significant displacement of the H12. In order to improve the overall picture of free energy profiles, we have also performed ABF calculations in the presence of the corepressor peptide SMRT.[26] This is particularly interesting because configurations of the H12 similar to those observed in corepressor-bound crystallographic models were observed in ABF simulations of ligand-free, ligand-bound, and coactivator-bound PPARγ LBDs, but with energies ∼30 kcal mol^{-1} greater than that of the agonist conformation, implying that they were not accessible. Therefore, the presence of the corepressor peptide must promote a large perturbation of the free energy surface to allow the antagonist H12 conformations to be sampled.

Simulations of the LBD bound to a corepressor were performed for PPARα, for which a crystallographic model is available.[26] The free energy surface obtained is shown in Figure 11A. The position of the global minimizer is shifted, and the regions of minimum energy of ligand-free and Rosiglitazone-bound PPARγ become prohibited, while the regions of high

DOI: 10.1021/acs.jpcb.5b09824
J. Phys. Chem. B 2015, 119, 15418−15429

energy sampled in previous runs are stabilized. Therefore, the corepressor stabilized conformations of the H12 which are not accessible in its absence, and promotes a relative increase in the free energies of the agonist H12 conformations.

There are overlaps between the subsets of conformation accessible in the presence of corepressor and those accessible in the absence of ligand. Structures very similar to C2 conformation are observed in corepressor-bound simulations (Figure 11B). This result suggests that the C2 conformation supports the interaction with the corepressor peptide. However, the antagonist conformation which is observed with the corepressor must still be stabilized by antagonist binding.

In the corepressor-bound system, the accessible free energy surface is very wide, and shows two local minima (Figure 12). One of the local minima corresponds to H12 conformations which are similar to the agonist conformations. Interestingly, this agonist, low-energy conformations, required the displacement of the corepressor peptide from the crystallographic position, as shown in Figure 12. In the crystallographic model, the SMRT peptide adopts a three-turn α-helix and docks into a hydrophobic groove formed by helices **3**, **4**, and **5**. Besides that, the corepresor helix is anchored to PPARα by hydrogen bonds between the Lys292 (from H3) and the CoR peptide, as shown in Figure 12B.[26] The rearrangement of H12 to restore the active conformation require dragging the corepressor peptide, notably with the disruption of its interaction with Lys292. The initial stages of this displacement are not thermodynamically prohibited, such that the LBD can assume a full agonist conformation in the presence of a partially displaced corepressor. Agonist binding, by stabilizing the H12 in the agonist structure, might therefore actively promote the dissociation of the corepressor.

Classification of the Conformational Equilibrium of the H12. The free energy profiles obtained here allow us to classify the conformational equilibria induced by the association of ligands and cofactors according to general models. Figure 13 summarizes our observations.

In the ligand-free receptor, multiple conformations of the H12 are accessible. The most stable conformation is the agonist conformation, but the helix is mobile. Not only multiple minima with small free energy differences are present, but the transitions between these minima are also of low energy. Indeed, the low free energy well is more clearly described as a rugged free energy landscape, spanning various conformations. A simplified free energy plot illustrating the multiple accessible states of the ligand-free receptor is shown in Figure 13A.

Ligand binding promotes a conformational selection. The agonist conformation of the H12 is stabilized relative to other conformations, as shown in Figure 13B. The ligand does not change the structural nature of the most stable conformation but makes of it the only accessible conformation at room temperature. Coactivator binding has a similar effect as that of ligand binding, and both effects might be additive. The agonist conformation is stabilized relative to other states, but the stabilization is more pronounced with the coactivator peptide. Therefore, it can also be classified as a conformational selection mechanism. Ligand or coactivator association causes the relative stabilization of the agonist conformation, without inducing conformational changes to the LBD to previously unaccessible states.

The association of the corepressor, on the other side, promotes a conformational transition of the H12 that cannot be anticipated from the accessible conformations of the ligand-free receptor. The favorable conformations in the presence of the corepressor are tenths of kcal mol^{-1} far from the stable corepressor-free conformers in the other free energy profiles. Therefore, the H12 can only assume these conformations induced by the association of the corepressor. The accessible conformations are also mutually exclusive, such that the ones that are accessible without the corepressor become prohibited when it is bound to the LBD. Nevertheless, small displacements of the corepressor with small energetic cost permit the H12 to assume conformations which are close to the agonist one. The simplified representation of the perturbation of the free energy surface introduced by the association of the corepressor is shown in Figure 13C. As the conformations assumed by the H12 in this case can only be observed after the association of the corepressor, the mechanism of repression is an induced-fit mechanism.

CONCLUSIONS

We have performed adaptive biasing-force molecular dynamics simulations to map the free energy profile of the conformational equilibrium of the Helix 12 of the PPARγ receptor. This conformational equilibrium is the most important factor controlling transcription activation or repression by NRs.

The free energy surfaces obtained allowed us to propose general models for ligand and cofactor related conformational changes on the receptor. Without ligand, the H12 is able to shift between various conformations, consistently with the experimental data that demonstrates its increased mobility. These conformations are, at the same time, always consistent with a compact receptor, thus no detachment of the H12 from the body of the receptor is expected. Furthermore, even in the absence of ligand, the most stable H12 conformation is the agonist conformation, providing a simple explanation for the basal activity of PPARγ. The accessibility of agonist H12 conformations in the absence of ligand was also recently demonstrated for the estrogen receptor,[25] supporting the generality of the results for the other members of the NR superfamily.

Ligand binding promotes a conformational selection. It stabilizes significantly the agonist H12 conformation relative to all other conformations which are accessible in the ligand-free receptor. A similar effect on the free energy surface is promoted by binding a coactivator peptide to the LBD. In both cases, the free energy well containing the agonist H12 is narrowed, and only conformations similar to that observed in the crystallographic model become accessible at room temperature. The stabilization of the agonist conformation by ligand binding exposes the coactivator binding surface permanently. The coactivator itself stabilizes the same conformation, such that it has an additive role for the stability of the active form of the LBD.

Corepressor binding, on the other side, perturbs completely the free energy surface. Conformations which are accessible in the ligand-free, in the presence of Rosiglitazone, or in the presence of the coactivator, become unfavorable. The favored conformations in the presence of the corepressor are those with a large displacement of the H12, and these are not accessible in other conditions. Therefore, the association of the corepressor induces a conformational transition in the protein, and the mechanism of repression follows an induced-fit model. Interestingly, however, the H12 can assume agonist-like conformations by displacing the corepressor peptide with a small energetic cost. As the ligand stabilizes the agonist

DOI: 10.1021/acs.jpcb.5b09824
J. Phys. Chem. B 2015, 119, 15418−15429

conformation, this might be the mechanism for the initial agonist-induced dissociation of the corepressor.

Therefore, in conjunction with previous experimental and simulation data, this work contributes to a definitive model of the conformational equilibrium of the most important switch for transcription activation of nuclear hormone receptors.

AUTHOR INFORMATION

Corresponding Author

*(L.M.) Telephone: +55 19 3521 3107. E-Mail: leandro@iqm.unicamp.br.

Notes

The authors declare no competing financial interest.

ACKNOWLEDGMENTS

The authors thank Fapesp and the Center for Computational Engineering and Sciences (CCES) (Grants 2010/16947-9, 2011/51348-1, 2013/05475-7, and 2013/09465-6), CNPq (Grants 304058/2013-0 and 470374/2013-6), and Faepex (Grant 596/13) for financial support.

REFERENCES

(1) Kumar, R.; Thompson, E. R. The Structure of the Nuclear Hormone Receptors. *Steroids* **1999**, *64*, 310−319.

(2) Aranda, A.; Pascual, A. Nuclear Hormone Receptor and Gene Expression. *Physiol. Rev.* **2001**, *81*, 1269−1304.

(3) Mackinnon, J. A. G.; Gallastegui, N.; Osguthorpe, D. J.; Hagler, A. T.; Estebanez-Perpina, E. E. Allosteric Mechanisms of Nuclear Receptors: Insights from Computational Simulations. *Mol. Cell. Endocrinol.* **2014**, *393*, 75−82.

(4) Bourguet, W.; Ruff, M.; Chambon, P.; Gronemeyer, H.; Moras, D. Crystal Structure of the Ligand-Binding Domain of the Human Nuclear Receptor RXRα. *Nature* **1995**, *375*, 377−382.

(5) Renaud, J. P.; Rochel, N.; Ruff, M.; Vivat, V.; Chambon, P.; Gronemeyer, H.; Moras, D. Crystal Structure of the RARγ Ligand-Binding Domain Bound to All Trans Retinoic. *Nature* **1995**, *378*, 681−689.

(6) Moras, D.; Gronemeyer, H. The Nuclear Receptor Ligand-Binding Domain: Structure and Function. *Curr. Opin. Cell Biol.* **1998**, *10*, 384−391.

(7) Gronemeyer, H.; Gustafsson, J. A.; Laudet, V. Principles for the Modulation of the Nuclear Receptor Superfamily. *Nat. Rev. Drug Discovery* **2004**, *3*, 950−964.

(8) Nettles, K. W.; Greene, G. L. Ligand Control of Coregulator Recruiment to Nuclear Receptors. *Annu. Rev. Physiol.* **2005**, *67*, 309−333.

(9) Wang, J.; Shao, Q.; Xu, Z.; Liu, Y.; Yang, Z.; Cossins, B. P.; Jiang, H.; Chen, K.; Shi, J.; Zhu, W. Exploring Transition Pathway and Free-Energy Profile of Large-Scale Protein Conformational Change by Combining Normal Mode Analysis and Umbrella Sampling Molecular Dynamics. *J. Phys. Chem. B* **2014**, *118*, 134−143.

(10) Koshland, D. E. Application of a Theory of Enzyme Specificity to Protein Synthesis. *Proc. Natl. Acad. Sci. U. S. A.* **1958**, *44*, 98−104.

(11) Bucher, D.; Grant, B. J.; Mccammon, J. A. Induced Fit or Conformational Selection? The Role of the Semi-Closed State in the Maltose Binding Protein. *Biochemistry* **2011**, *50*, 10530−10539.

(12) Martínez, L.; Sonoda, M. T.; Webb, P.; Baxter, J. D.; Skaf, M. S.; Polikarpov, I. Molecular Dynamics Simulations Reveal Multiple Pathways of Ligand Dissociation from Thyroid Hormone Receptors. *Biophys. J.* **2005**, *89*, 2011−2023.

(13) Rastinejad, F.; Ollendorff, V.; Polikarpov, I. Nuclear Receptor Full-Length Architectures: Confronting Myth and Illusion With high Resolution. *Trends Biochem. Sci.* **2015**, *40*, 16−24.

(14) Tanenbaum, D. M.; Wang, Y.; Williams, S. P.; Sigler, P. B. Crystallographic Comparison of the Estrogen and Progesterone Receptor's Ligand Binding Domains. *Proc. Natl. Acad. Sci. U. S. A.* **1998**, *95*, 5998−6003.

(15) Nolte, R. T.; Wisely, G. B.; Westin, S.; Cobb, J. E.; Lambert, M. H.; Kurokawa, R.; Rosenfeld, M. G.; Willson, T. M.; Glass, C. K.; Milburn, M. V. Ligand Binding and Co-activator Assembly of the Peroxisome Proliferator-Actived Receptor-γ. *Nature* **1998**, *395*, 137−143.

(16) Wang, Y.; Chirgadze, N. Y.; Briggs, S. L.; Khan, S.; Jensen, E. V.; Burris, T. P. A Second Binding Site for the Hydroxytamoxifen Within the Coactivator-Binding Groove of Estrogen Receptor β. *Proc. Natl. Acad. Sci. U. S. A.* **2006**, *103*, 9908−9911.

(17) Figueira, A. C. M.; Saidemberg, D. M.; Souza, P. C. T.; Martínez, L.; Scanlan, T. S.; Baxter, J. D.; Skaf, M. S.; Palma, M. S.; Webb, P.; Polikarpov, I. Analysis of Agonist and Antagonist Effects on Thyroid Hormone Receptor Conformation by Hydrogen/Deuterium Exchange. *Mol. Endocrinol.* **2011**, *25*, 15−31.

(18) Blondel, A.; Renaud, J. P.; Fischer, S.; Moras, D.; Karplus, M. Retinoic Acid Receptor: A Simulation Analysis of Retinoic Acid Binding and the Resulting Conformational Changes. *J. Mol. Biol.* **1999**, *291*, 101−115.

(19) Kosztin, D.; Izrailev, S.; Schulten, K. Unbinding of Retinoic Acid From Its Receptor Studied by Steered Molecular Dynamics. *Biophys. J.* **1999**, *76*, 188−197.

(20) Martínez, L.; Webb, P.; Polikarpov, I.; Skaf, M. S. Molecular Dynamics Simulations of Ligand Dissociation From Thyroid Hormone Receptors: Evidence of the Likeliest Escape Pathway and Its Implications for the Design of Novel Ligands. *J. Med. Chem.* **2006**, *49*, 23−26.

(21) Martínez, L.; Polikarpov, I.; Skaf, M. S. Only Subtle Protein Conformational Adaptations Are Require for Ligand Binding to Thyroid Hormone Receptors: Simulations Using a Novel Multipoint Steered Molecular Dynamics Approach. *J. Phys. Chem. B* **2008**, *112*, 10741−10751.

(22) Souza, P. C. T.; Barra, G. B.; Velasco, L. F.; Ribeiro, I. C.; Simeoni, L. A.; Togashi, M.; Webb, P.; Neves, F. A. R.; Skaf, M. S.; Martínez, L.; et al. Helix 12 Dynamics and Thyroid Hormone Receptor Activity: Experimental and Molecular Dynamics Studies of Ile280 Mutants. *J. Mol. Biol.* **2011**, *412*, 882−893.

(23) Fratev, F.; Tsakovska, I.; Al Sharif, M.; Mihaylova, E.; Pajeva, I. Structural and Dynamical Insights into PPARγ Antagonism: In Silico Study of the Ligand-Receptor Interactions of Non-Covalent Antagonists. *Int. J. Mol. Sci.* **2015**, *16*, 15405−15424.

(24) Batista, M. R. B.; Martínez, L. Dynamics of Nuclear Receptor Helix-12 Switch of Transcription Activation by Modeling Time-Resolved Fluorescence Anisotropy Decays. *Biophys. J.* **2013**, *105*, 1670−1680.

(25) Fratev, F. Helix 12 Orientation in Estrogen Receptors is Mediated by Receptor Dimerization: Evidence from Molecular Dynamics Simulations. *Phys. Chem. Chem. Phys.* **2015**, *17*, 13403−13420.

(26) Xu, H. E.; Stanley, T. B.; Montana, V. G.; Lambert, M. H.; Shearer, B. G.; Cobb, J. E.; McKee, D. D.; Galardi, C. M.; Plunket, K. D.; Nolte, R. T.; et al. Structural Basis for Antagonist-Mediated Recruiment of Nuclear Co-repressors by PPARα. *Nature* **2002**, *415*, 813−817.

(27) Martínez, J. M.; Martínez, L. Packing Optimization for Automated Generation of Complex System's Initial Configurations for Molecular Dynamics and Docking. *J. Comput. Chem.* **2003**, *24*, 819−825.

(28) Martínez, L.; Andrade, R.; Birgin, E. G.; Martínez, J. M. Packmol: A Package for Building Initial Configurations for Molecular Dynamics Simulations. *J. Comput. Chem.* **2009**, *30*, 2157−2164.

(29) Mackerell, A. D.; Bashford, D.; Bellott, M.; Dunbrack, R. L.; Evanseck, J. D.; Field, M. J.; Fischer, S.; Gao, J.; Guo, H.; Ha, S.; et al. All Atom Empirical Potential for Molecular Modeling and Dynamics Strudies of Protein. *J. Phys. Chem. B* **1998**, *102*, 3586−3616.

(30) Hansson, A.; Souza, P. C. T.; Silveira, R. L.; Martínez, L.; Skaf, M. S. Charmm Force Field Parametrization of Rosiglitazone. *Int. J. Quantum Chem.* **2011**, *111*, 1346−1354.

DOI: 10.1021/acs.jpcb.5b09824
J. Phys. Chem. B 2015, 119, 15418−15429

(31) Jorgensen, W. L.; Chandrasekhar, J.; Madura, J. D.; Impey, R. W.; Klein, M. L. Comparison of simple potential functions for simulating liquid water. *J. Chem. Phys.* **1983**, *79*, 926−935.
(32) Phillips, J. C.; Braun, R.; Wang, W.; Gumbart, J.; Tajkhorshid, E.; Villa, E.; Chipot, C.; Skeel, R. D.; Kalè, L.; Schulten, K. Scalable Molecular Dynamics with Namd. *J. Comput. Chem.* **2005**, *26*, 1781−1802.
(33) Humphrey, W.; Dalke, A.; Schulten, K. Vmd: Visual Molecular Dynamics. *J. Mol. Graphics* **1996**, *14*, 33−38.
(34) Shao, J.; Tanner, S. W.; Thompson, N.; Cheatham, T. E. Clustering Molecular Dynamics Trajectories: 1. Characterizing the Performance of Different Clustering Algorithms. *J. Chem. Theory Comput.* **2007**, *3*, 2312−2334.
(35) Arrar, M.; Turnham, R.; Pierce, L.; de Oliveira, C. A. F.; Mccammon, J. A. Structural Insight into the Separate Roles of Inositol Tetraphosphate and Deacetylase-Activating Domain in Activation of Histone Deacetylase 3. *Protein Sci.* **2013**, *22*, 83−92.
(36) Henin, J.; Chipot, C. Overcoming Free Energy Barriers Using Unconstrained Molecular Dynamics Simulations. *J. Chem. Phys.* **2004**, *121*, 2904−2914.
(37) Chipot, C.; Henin, J. Exploring the Free-Energy Landscape of a Short Peptide Using an Average Force. *J. Chem. Phys.* **2005**, *123*, 244906−244911.
(38) Chipot, T.; Lelievre, T. Enhanced Sampling of Multidimensional Free-Energy Landscapes Using Adaptive Biasing Forces. *SIAM J. Appl. Math.* **2011**, *71*, 1673−1695.
(39) Darve, E.; Rodriguez-Gomez, D.; Pohorille, A. Adaptive Biasing Force Method for Scalar and Vector Free Energy. *J. Chem. Phys.* **2008**, *128*, 144120−144134.
(40) Comer, J.; Gumbart, J. C.; Hénin, J.; Lelievre, T.; Pohorille, A.; Chipot, C. The Adaptive Biasing Force Method: Everything You Always Wanted To Know but Were Afraid To Ask. *J. Phys. Chem. B* **2015**, *119*, 1129−1151.
(41) Kallenberger, B. C.; Love, J. D.; Chatterjee, V. K. K.; Schwabe, J. W. R. A Dynamic Mechanism of Nuclear Receptor Activation and Its Perturbation in Human Disease. *Nat. Struct. Biol.* **2003**, *10*, 136−140.
(42) Nagy, L.; Schwabe, J. Mechanism of the Nuclear Receptor Molecular Switch. *Trends Biochem. Sci.* **2004**, *29*, 317−324.
(43) Johnson, B. A.; Wilson, E. M.; Li, Y.; Moller, D. E.; Smith, R. G.; Zhou, G. Ligand-Induced Stabilization of PPARγ Monitored by NMR Spesctroscopic: Implications for Nuclear Receptor Activation. *J. Mol. Biol.* **2000**, *298*, 187−194.
(44) Hughes, T. S.; Chalmers, M. J.; Novick, S.; Kuruvilla, D. S.; Chang, M. R.; Kamenecka, T. M.; Rance, M.; Johnson, B. A.; Burris, T. P.; Griffin, P. R.; et al. Ligand and Receptor Dynamics Contribute To the Mechanism of Graded PPARγ Agonism. *Structure* **2012**, *20*, 139−150.
(45) Zoete, V.; Grosdidier, A.; Michielin, O. Peroxissome Proliferator-Actived Receptor Structures: Ligand Specificity, Molecular Switch and Interactions with Regulators. *Biochim. Biophys. Acta, Mol. Cell Biol. Lipids* **2007**, *1771*, 915−925.
(46) Molnar, F.; Matilainen, M.; Carlberg, C. Structural Determinants of the Agonist-Independent Association of Humam Peroxisome Proliferator Activated Receptors with Coactivators. *J. Biol. Chem.* **2005**, *280*, 26543−26556.
(47) Gurnell, M.; Wentworth, J. M.; Agostini, M.; Adams, M.; Collingwood, T. N.; Provenzano, C.; Browne, P. O.; Rajanayagam, O.; Burris, T. P.; Schwabe, J. W.; et al. A Dominant Negative Peroxisome Proliferator-Activated Receptor Gamma Mutant Is a Constitutive Repressor and Inhibits PPARγ-Mediated Adipogenesis. *J. Biol. Chem.* **2000**, *275*, 5754−5759.
(48) Bruning, J. B.; Chalmers, M. J.; Prasad, S.; Busby, S. A.; Kamenecka, T. M.; Nettles, K. W.; Griffin, P. R.; He, Y. Partial Agonists Activate PPARγ Using Helix 12 Independent Mechanism. *Structure* **2007**, *15*, 1258−1271.
(49) Waku, T.; Shiraki, T.; Oyama, T.; Maebara, K.; Nakamori, R.; Morikawa, K. The nuclear Receptor PPARγ Individually Responds To Serotonin and Fatty Acid-Metabolites. *EMBO J.* **2010**, *29*, 3395−3407.
(50) Montanari, R.; Saccoccia, F.; Scotti, E.; Crestani, M.; Godio, C.; Gilardi, F.; Loiodice, F.; Fracchiolla, G.; Laghezza, A.; Tortorella, P.; et al. Crystal Structure of the Peroxisome Proliferator-Activated Receptor γ (PPARγ) Ligand Binding Domain Complexed With a Novel Partial Agonist: A New Region of the Hydrophobic Pocket Could Be Exploited For Drug Design. *J. Med. Chem.* **2008**, *51*, 7768−7776.

DOI: 10.1021/acs.jpcb.5b09824
J. Phys. Chem. B 2015, 119, 15418−15429